Magnetic Coupling in End-to-End Azido-Bridged Copper and Nickel Binuclear Complexes: A Theoretical Study

Fabrizia Fabrizi de Biani,[‡] Eliseo Ruiz,[†] Joan Cano,[§] Juan J. Novoa,[||] and Santiago Alvarez*,[†]

Departament de Química Inorgànica, Departament de Química Física, and Centre de Recerca en Química Teòrica, Universitat de Barcelona, Diagonal 647, 08028 Barcelona, Spain, and Departament de Química Inorgànica, Universitat de València, Dr. Moliner 50, Burjassot, Valencia, Spain

Received January 5, 2000

The influence of structural parameters on the exchange coupling *J* between metal atoms in end-to-end azido-bridged binuclear complexes of Cu(II) and Ni(II) has been studied by means of density functional calculations. For the case of double-bridged Cu(II) compounds, four ideal pentacoordinate models have been employed in which the coordination spheres of the two metal atoms are either a trigonal bipyramid or a square pyramid, connected through equatorial or axial bridges. The distortion from those ideal geometries along a Berry pathway has also been analyzed. For the hexacoordinate Ni(II) compounds, models with two or one bridging ligands have been studied. The effect of the bridging M−N−N bond angles on the exchange coupling has been analyzed for both the Cu(II) and Ni(II) complexes.

One of the most appealing properties of binuclear transition metal complexes is the possible appearance of exchange interactions between the metal centers. The design of molecule-based magnets relies on the presence of both intra- and intermolecular coupling. Therefore, the inspection of the structural features which correlate with the strength and the sign of this interaction clearly constitutes a necessary first step in this direction.

Among binuclear complexes, those with azido ligands are particularly interesting due to their ability to act not only as monodentate ligands,[1−3] but also in end-on (**1a**) or end-to-end (**1b**) bridging coordination modes. Low-dimensional networks

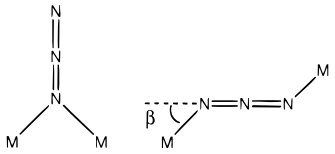

1a **1b**

can also be obtained in which the different coordination modes of the azido ligand coexist in the same structure.[4−7] The azido-bridged binuclear complexes provide a stringent test for any theoretical analysis of the exchange coupling, because they usually present ferromagnetic coupling in the end-on bridging mode, but antiferromagnetic interaction in the end-to-end bridging mode. In a recent publication, we presented a study on the exchange interaction between two M(II) ions (for M = Cu, Ni, Mn) in end-on azido-bridged complexes.[8] In that study we found that the computational methodology we applied reproduces, with reasonable accuracy, the experimental values of the coupling constant when the full molecular structure is included in the calculations. We also explored the effect of geometrical parameters on the coupling constant, and the predictions of our calculations, including the possibility of antiferromagnetic coupling with end-on bridged complexes of Mn(II) and of stronger ferromagnetic coupling in Cu(II) complexes, have been confirmed by recent experimental results.[5,9] Density functional calculations on the end-on bridged Cu(II) complexes have also been reported recently by Adamo et al.[10] To complete the picture we decided to undertake a similar study of the end-to-end azido-bridged complexes.

In this paper we report the results of a theoretical study on the end-to-end Cu(II) and Ni(II) complexes for which we used methods based on density functional theory (DFT). In our study, the values of the exchange coupling constant, *J*, are calculated at different geometries for the model complexes $[(NH_3)_6Cu_2(\mu\text{-}1,3\text{-}N_3)_2]^{2+}$, $[(NH_3)_8Ni_2(\mu\text{-}1,3\text{-}N_3)_2]^{2+}$, and $[(NH_3)_{10}Ni_2(\mu\text{-}1,3\text{-}N_3)]^{3+}$, as well as for the experimental structures of three

[†] Department de Química Inorgànica and Centre de Recerca en Química Teòrica, Universitat de Barcelona.

[‡] Permanent address: Universitá di Siena, Dipartimento di Chimica, via A. Moro, 53100 Siena, Italy.

[§] Universitat de València.

[||] Departament de Química Física and Centre de Recerca en Química Teòrica, Universitat de Barcelona.

(1) Kahn, O.; Pei, Y.; Journaux, Y. In *Inorganic Materials*, 2nd ed.; Bruce, Q. W., O'Hare, D., Eds.; J. Wiley: Chichester, U.K., 1997.
(2) Chaudhuri, P.; Weyhermüller, T.; Bill, E.; Wieghardt, K. *Inorg. Chim. Acta* **1996**, *252*, 195.
(3) Peñalba-Marina, E. Ph.D. Thesis, Universitat de Barcelona, Barcelona, Spain, 1998.
(4) Viau, G.; Lombardi, M. G.; De Munno, G.; Julve, M.; Lloret, F.; Faus, J.; Caneschi, A.; Clemente-Juan, J. M. *Chem. Commun.* **1997**, 1195.
(5) Vicente, R.; Escuer, A.; Ribas, J.; Solans, X. *Inorg. Chem.* **1992**, *31*, 1726.
(6) Escuer, A.; Vicente, R.; Ribas, J.; El Fallah, M. S.; Solans, X. *Inorg. Chem.* **1993**, *32*, 1033.
(7) Ribas, J.; Monfort, M.; Solans, X.; Drillon, M. *Inorg. Chem.* **1994**, *33*, 742.
(8) Ruiz, E.; Cano, J.; Alvarez, S.; Alemany, P. *J. Am. Chem. Soc.* **1998**, *120*, 11122.
(9) Goher, M. A. S.; Cano, J.; Journaux, Y.; Abu-Youssef, M. A. M.; Mautner, F. A.; Escuer, A.; Vicente, R. *Chem.−Eur. J.* **2000**, *6*, 778.
(10) Adamo, C.; Barone, V.; Bencini, A.; Totti, F.; Ciofini, I. *Inorg. Chem.* **1999**, *38*, 1996.
(11) Escuer, A.; Font-Bardía, M.; Peñalba, E.; Solans, X.; Vicente, R. *Inorg. Chim. Acta* **2000**, *298*, 195.
(12) Felthouse, T. R.; Hendrickson, D. N. *Inorg. Chem.* **1978**, *17*, 444.
(13) Chaudhuri, P.; Oder, K.; Wieghardt, K.; Nuber, B.; Weiss, J. *Inorg. Chem.* **1986**, *25*, 2818.

10.1021/ic000005x CCC: $19.00
Published on Web 06/24/2000

Table 1. Experimental Structural Data[a] and Exchange Coupling Constants[b] for End-to-End Azido-Bridged Cu(II) Binuclear Complexes

	compound[c]	δ	τ[d]	S(tbp)[e]	Cu−N_b−N	N_b−Cu−N_b	J_{exp}	J_{calc}	ref
A[f]	$[Cu_2(\mu\text{-}N_3)_2(Et_5dien)_2]^{2+}$		0.43	2.82	126−127	88			11
			0.43	2.84	129−137	89	−28		11
B	$[Cu_2(\mu\text{-}N_3)_2(Et_5dien)_2](BPh_4)_2$	0	0.29	3.16	124−140	93	−13		12
C	$[Cu_2(\mu\text{-}N_3)_2(EtMe_4dien)_2]^{2+}$	16	0.28	3.43	123−138	91	−3.6		11
D	$[Cu_2(\mu\text{-}N_3)_2(Me_5dien)_2](ClO_4)_2$	16	0.23	3.76	123−138	92	−7.5	6.6	11
E	$[Cu_2(\mu\text{-}N_3)_2(Et_3dien)_2]^{2+}$	18	0.20	4.25	124−138	88	9.0	7.6	3
F	$[Cu_2(\mu\text{-}N_3)_2(tmtacn)_2]^{2+}$	7	0.05	6.33	128−132	93	<−800	−1270	13
G	$[Cu_2(\mu\text{-}N_3)_2(24\text{-ane-}N_2S_4)_2]$	0			127−136	92	<−1000		14,15

[a] Compounds **A**−**E** present structures intermediate between aSP and aTBP, compound **F** has an eSP structure, and compound **G** has hexacoordinate copper ions. [b] All distances in Å, angles in deg, J in cm^{-1}. [c] See ref 51 for abbreviations used in this table. [d] Addison parameter (ref 20). [e] Continuous symmetry measure (ref 22). [f] Two independent molecules in the asymmetric unit. The torsion angle δ is not defined.

Cu(II) complexes. For these families of compounds, the wide range of experimental J values (Table 1) is noteworthy and indicates the high sensitivity of the exchange interaction to small structural changes. All J values reported in this paper correspond to the spin Hamiltonian $H = -J\mathbf{S}_1\cdot\mathbf{S}_2$.

Double-Bridged Cu(II) Complexes

Cu(II) Binuclear Compounds with Idealized Structures. To the best of our knowledge, practically all of the end-to-end azido-bridged Cu(II) complexes are pentacoordinate (Table 1, compounds **A**−**E**). The only exception is a complex of the macrocyclic ligand [24-ane-N_2S_4] in which the copper ions are in a highly distorted octahedral environment[14,15] (Table 1, compound **G**). Because of its exceptionality, this kind of structure will not be further discussed in this work, and we will concentrate on the study of binuclear complexes with pentacoordinate Cu(II) ions and two azido bridges. The two ideal coordination geometries for pentacoordination are the square pyramid (SP) and the trigonal bipyramid (TBP). The orbital bearing the unpaired electron in a pentacoordinated Cu(II) atom has a different nature in each case. In the square pyramid it is an x^2-y^2 type orbital, parallel to the base of the pyramid (**2a**). In the trigonal bipyramid, the semioccupied orbital is of the z^2 type, directed along the trigonal axis (**2b**). The real coordination

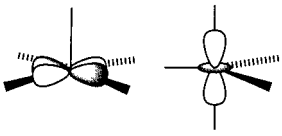

2a **2b**

around Cu(II) is usually found to be intermediate between a square pyramid and a trigonal bipyramid, but we concentrate first on the ideal geometries. In a later section we will discuss the intermediate geometries.

The combination of two pentacoordinate metal atoms in a bis(azido)-bridged binuclear complex can result in a variety of possible structures, depending on the local coordination of each metal atom and the equatorial or axial position of the bridging azido ligands. The simplest structures, shown in **3**, are those in which the two metal atoms have identical coordination spheres. Those geometries will be referred to hereinafter with a lower case letter indicating the position of the bridging ligands (e for equatorial, a for axial) and upper case letters to indicate the local coordination spheres (SP for square pyramid, TBP for trigonal bipyramid). Our calculations of energies for the model compound $[Cu_2(\mu\text{-}N_3)_2(NH_3)_6]^{2+}$ with such idealized structures

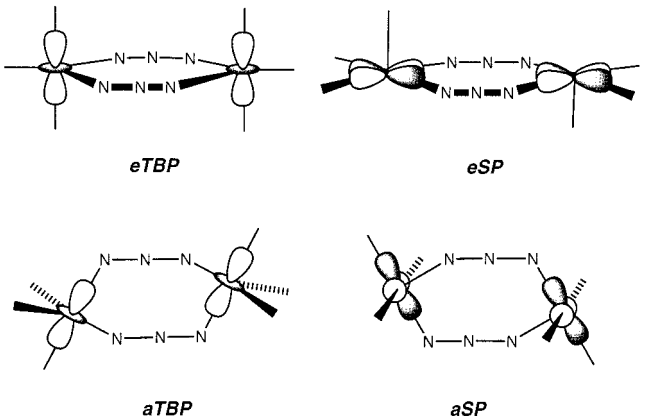

3

indicate that the aSP, eSP, and aTBP isomers differ by less than 5 kcal/mol, whereas the eTBP structure is 27 kcal/mol higher than aSP. These results are consistent with the experimental existence of five compounds with geometries intermediate between aSP and aTBP (Table 1, compounds **A**−**E**) and of one compound with eSP structure (Table 1, compound **F**), whereas no eTBP structure has so far been reported.

The calculated values for the exchange coupling parameter, J, for the four regular models (**3**) are presented in Table 2. The influence of the geometry on the coupling constant is remarkable, because the calculations predict a variety of magnetic behaviors, from ferromagnetic for aSP to practically diamagnetic for *eSP*. The only known compound with an *eSP* structure is diamagnetic at room temperature (Table 2, compound **F**), in excellent agreement with the large negative value calculated for the coupling constant of the regular model. Experimentally known compounds with structures between aTBP and aSP present small negative values of J (Table 1, compounds **A**−**E**), well within the range expected for the two extreme cases (−345 and +32 cm^{-1} for aTBP and aSP, respectively). A similar behavior was found for binuclear Cu(II) oxalato-bridged derivatives,[16] for which orbital topologies comparable to *eSP*, aSP, and aTBP are calculated to give J values of −293, +10, and −185 cm^{-1}, respectively.

According to the theoretical analysis presented by Hay, Thibeault, and Hoffmann,[17] in a binuclear complex with two unpaired electrons described by molecular orbitals ϕ_1 and ϕ_2, the coupling constant can be approximated by eq 1. There, ϵ_1 and ϵ_2 are the orbital energies, K_{ab} is the exchange integral between two localized orbitals obtained as linear combinations of ϕ_1 and ϕ_2, and J_{aa} and J_{ab} are the corresponding Coulomb

(14) Agnus, Y.; Louis, R.; Weiss, R. *J. Am. Chem. Soc.* **1979**, *101*, 3381.
(15) Agnus, Y.; Louis, R.; Gisselbrecht, J. P.; Weiss, R. *J. Am. Chem. Soc.* **1984**, *106*, 93.
(16) Cano, J.; Alemany, P.; Alvarez, S.; Verdaguer, M.; Ruiz, E. *Chem.−Eur. J.* **1998**, *4*, 476.
(17) Hay, P. J.; Thibeault, J. C.; Hoffmann, R. *J. Am. Chem. Soc.* **1975**, *97*, 4884.

Table 2. Calculated Parameters[a] (UB3LYP) for the Ideal Geometries (**3**) of the Model Compound $[Cu_2(\mu\text{-}N_3)_2(NH_3)_6]^{2+}$

	eSP	aTBP	eTBP	aSP
J_{calcd}	−1 036	−345	−291	32
$\epsilon_1 - \epsilon_2$	15 300	647	9 050	1 550
$2K_{ab}$	7 357	130	6 753	891
$J_{aa} - J_{ab}$	21 157	62 809	23 812	28 257

[a] All values in cm^{-1}.

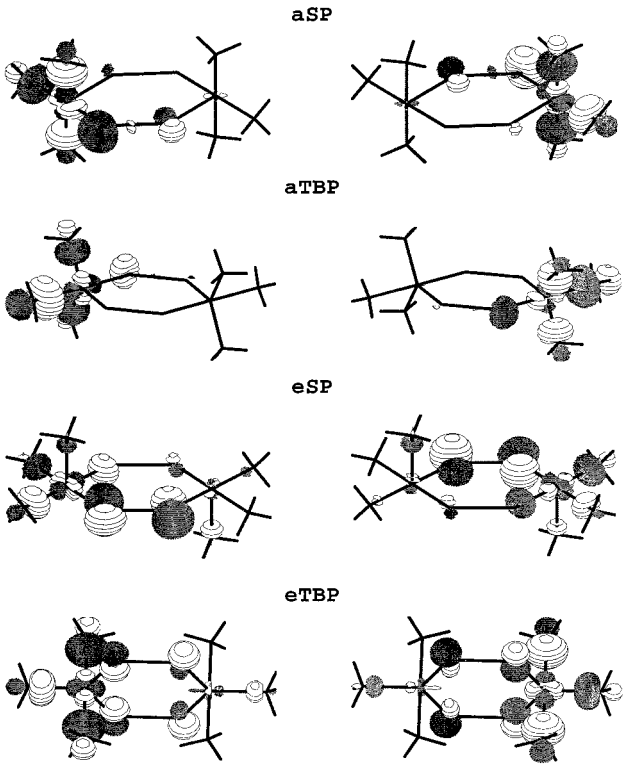

Figure 1. Localized molecular orbitals obtained as sum and difference of the two SOMOs of $[Cu_2(\mu\text{-}N_3)_2(NH_3)_6]^{2+}$ in the four idealized geometries (see **3**), as obtained from B3LYP calculations on its triplet state.

integrals. The first term ($2K_{ab}$) is positive and can be considered the ferromagnetic contribution to the exchange coupling, whereas the second term is negative and represents the antiferromagnetic contribution.

$$E_S - E_T = J = 2K_{ab} - \frac{(\epsilon_1 - \epsilon_2)^2}{J_{aa} - J_{ab}} \qquad (1)$$

Assuming that the two-electron terms (K_{ab}, J_{aa}, and J_{ab}) are approximately constant within a family of related compounds, changes in the coupling constant are usually interpreted as reflecting the differences in the orbital gap ($\epsilon_1 - \epsilon_2$). Our findings for a variety of binuclear complexes show that a practically linear correlation is found between the calculated J and the square of the orbital gap,[18,19] but such a correlation does not exist in the present case as can be seen by comparing the values of the same parameters for the aTBP and aSP structures (Table 2). In particular, the aTBP structure presents a value of $(\epsilon_1 - \epsilon_2)^2$ much smaller (4.1×10^5 cm^{-2}) than those values found for previously studied compounds or for the eSP and eTBP geometries ($\sim 10^7 - 10^8$ cm^{-2}), but still the calculated coupling is quite strongly antiferromagnetic. In an attempt to unravel the reasons for such anomalous behavior, we have undertaken the calculation of the two-electron terms K_{ab}, J_{aa}, and J_{ab} corresponding to the localized version of the Kohn−Sham SOMOs in the triplet state (see the Appendix for details). Given the approximations involved in the derivation of eq 1, one should not ascribe undue confidence to the numerical values reported, especially taking into account that in some cases there are several occupied orbitals with the same symmetry and there is some arbitrariness in deciding which one should be considered as a SOMO on which to apply eq 1, for which only one symmetric orbital and one antisymmetric orbital were considered. However, we expect that the trends in the analyzed parameters bear a close relationship with the physical reality they try to describe and can thus provide us with plausible explanations for the differences in the calculated J values.

To test the reliability of the two-electron integrals calculated with the UB3LYP method, we have repeated the calculations for the four idealized models at the UHF and ROHF levels of theory. The localization of the molecular orbitals obtained from the UHF calculations is quite similar to that found with UB3LYP, whereas the ROHF method produces very different orbital localization, thereby resulting in a very different ordering of, e.g., the K_{ab} integral for the four models. This result is not unexpected, because the restricted approach assumes the same spatial functions for the α and β spins of each electron pair, whereas the unrestricted approach allows for different spatial distribution of the molecular orbitals associated with α and β electrons in order to maximize the exchange integrals. Although we still do not have a thorough understanding of the values that may adopt the two-electron terms in eq 1 and the factors that affect them, the present results give us hope that by calculation we eventually will be able to design molecular systems with the desired type and magnitude of exchange coupling.

The calculated values of K_{ab} (Table 2) clearly indicate that the ferromagnetic contribution in the aTBP structure is much smaller than in the rest of the models, explaining why, even with a small gap, the net interaction is antiferromagnetic. Not only are the values of the calculated exchange integrals consistent with the anomalous gap dependence of the coupling constant, but the trends in the values of K_{ab} can be easily understood from the topology of the SOMOs in each case (Figure 1). Because K_{ab} integrates products of the type $\psi_a(1)\psi_b(2)$ at each point in space, large values of K_{ab} should be expected when ψ_a and ψ_b have significant contributions of atomic orbitals centered at the same atoms. When ψ_a and ψ_b are located at different atoms (disjoint functions), small values of K_{ab} should be expected. The present results indicate that attempts to explain trends in the exchange coupling constant by analyzing the orbital gap should be made with extreme caution when comparing structures for which the SOMOs are expected to present different topologies.

Puckering of the CuN_3CuN_3 Ring in aSP and aTBP Structures. In the model calculations discussed above, we have assumed that the CuN_3CuN_3 ring is planar, but it deviates significantly from the planarity of the experimental structures. Hence, it is worth studying the effect of ring puckering on the coupling constant J. Because the azido ligands are practically linear, we can measure the degree of ring puckering by two

(18) Cano, J.; Ruiz, E.; Alemany, P.; Lloret, F.; Alvarez, S. *J. Chem. Soc., Dalton Trans.* **1999**, 1669.
(19) Alvarez, S.; Palacios, A. A.; Aullón, G. *Coord. Chem. Rev.* **1999**, *185−186*, 431.

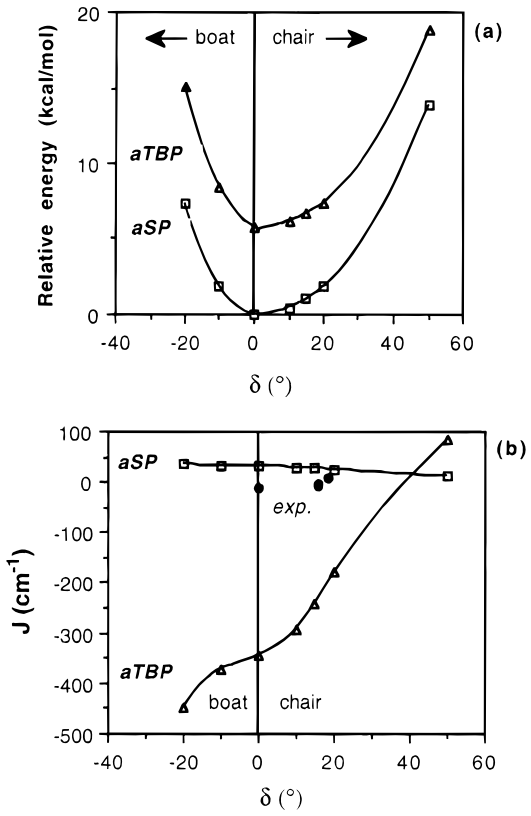

Figure 2. (a) Calculated energy of $[Cu_2(\mu\text{-}N_3)_2(NH_3)_6]^{2+}$ in its lowest-energy spin state, represented as a function of the degree of ring distortion δ (see **4**). (b) Calculated J (cm^{-1}) as a function of δ for the aSP (squares) and aTBP (triangles) structures. Experimental data for binuclear Ni(II) complexes with two 1,3-azido bridges (closed circles) are also shown for comparison.

dihedral angles: that between the two N_3 groups, χ (**5**), and

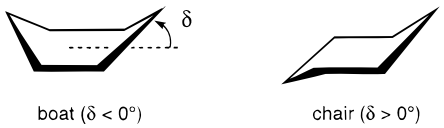

4

that between the N_6 and CuN_2 planes, δ (**4**). Although the first

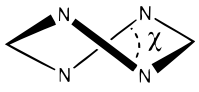

5

type of distortion is sometimes found in Ni azido complexes,[3] the two azido bridges are practically parallel in Cu(II) derivatives, with the only exception being compound **A** (Table 1). The copper atoms are often out of the plane formed by the two azido ligands, resulting in a chair conformation with dihedral angles δ as large as 20°, whereas no structure with the boat conformation has been reported so far. Consequently, we analyze in this section the influence of only the dihedral angle δ. For convenience, we will represent the chair conformation by positive values of δ and the boat conformation by negative δ values (**4**).

To analyze the effect of ring puckering on the exchange coupling we consider the axially bridged structures of the model complex $[Cu_2(\mu\text{-}N_3)_2(NH_3)_6]^{2+}$. In Figure 2a we show the relative energies of the calculated ground states for the aSP (triplet) and the aTBP (singlet) geometries as a function of δ. The results indicate that the optimum geometry is the coplanar one ($\delta = 0°$) in the two cases, but a chair distortion requires only 2 kcal/mol for δ values as high as 20°. In contrast, a similar boat distortion requires 7 kcal/mol, in agreement with the experimental occurrence of chair conformations only. The present results also suggest that the preferred conformation of the multidentate ligands, or other second coordination sphere interactions (e.g., ligand sterics, hydrogen bonding, or interactions with counterions), may be sufficient to account for the experimental occurrence of ring puckering in the chair conformation.

The calculated values of J as a function of δ are presented in Figure 2b. It is interesting to note that the ring puckering has a strong influence on the exchange coupling constant for the aTBP geometry, but has a small effect on the exchange coupling constant for the aSP structure. In the former case, the chair and boat distortions have opposite effects on the calculated J: while a chair distortion decreases the antiferromagnetic coupling, eventually producing ferromagnetic behavior for large δ values, a boat distortion increases the antiferromagnetic character of the exchange. For the aTBP case, the value of J remains small and positive regardless of the degree of ring puckering. In agreement with such results, the experimental data for axially bridged complexes (Table 1, **A**−**E**) with structure types intermediate between aSP and aTBP give values of J intermediate between those expected for the two extreme structures. Furthermore, the experimental J values are not correlated with the degree of ring puckering (Figure 3), as predicted for the aSP form. In conclusion, the geometry of the coordination sphere around the Cu atoms seems to be much more important in determining the value of J than the degree of ring puckering, and a study of the evolution of J along the interconversion of the Cu(II) coordination sphere from TBP to SP is addressed in the next section.

Interconversion between aTBP and aSP Geometries. Because the Cu atoms present coordination geometries intermediate between SP and TBP, in the experimental structures, we study in more detail the effect that a distortion from regular square pyramid to a regular trigonal bipyramid has on the calculated exchange coupling constant. For the subsequent discussion we need to identify the degree of proximity of any structure to the two ideal geometries. The angular parameter,[20] τ, proposed by Addison et al. is often used for such a purpose. That parameter is defined as $\tau = |\beta - \alpha|/60$ (where α and β are the two largest L−M−L bond angles), so that $\tau = 1$ for a trigonal bipyramid and $\tau = 0$ for a square pyramid. An alternative parameter that can be considered is the continuous symmetry measure defined by Avnir and co-workers.[21,22] In essence, these authors devised a method whereby the deviation of a given molecular structure from an idealized polyhedron can be defined by a single parameter. In the present case we use the continuous symmetry measure of a trigonal bipyramid, S(tbp), that must be zero for a perfect trigonal bipyramid and increases as the polyhedron deviates from the D_{3h} symmetry. Although the maximum possible value of S(tbp) is 100, a study of the continuous symmetry measure in pentacoordinate transition metal complexes[23] shows that the values for a square

(20) Addison, A. W.; Rao, T. N.; Reedijk, J.; van Rijn, J.; Verschoor, G. C. *J. Chem. Soc., Dalton Trans.* **1984**, 1349.
(21) Avnir, D.; Katzenelson, O.; Keinan, S.; Pinsky, M.; Pinto, Y.; Salomon, Y.; Zabrodsky Hel-Or, H. In *Concepts in Chemistry;* Rouvray, D. H., Ed.; Research Studies Press: Taunton, Somerset, U.K., 1997; Chapter 9.
(22) Pinsky, M.; Avnir, D. *Inorg. Chem.* **1998**, *37*, 5575.
(23) Alvarez, S.; Llunell, M., to be submitted for publication.

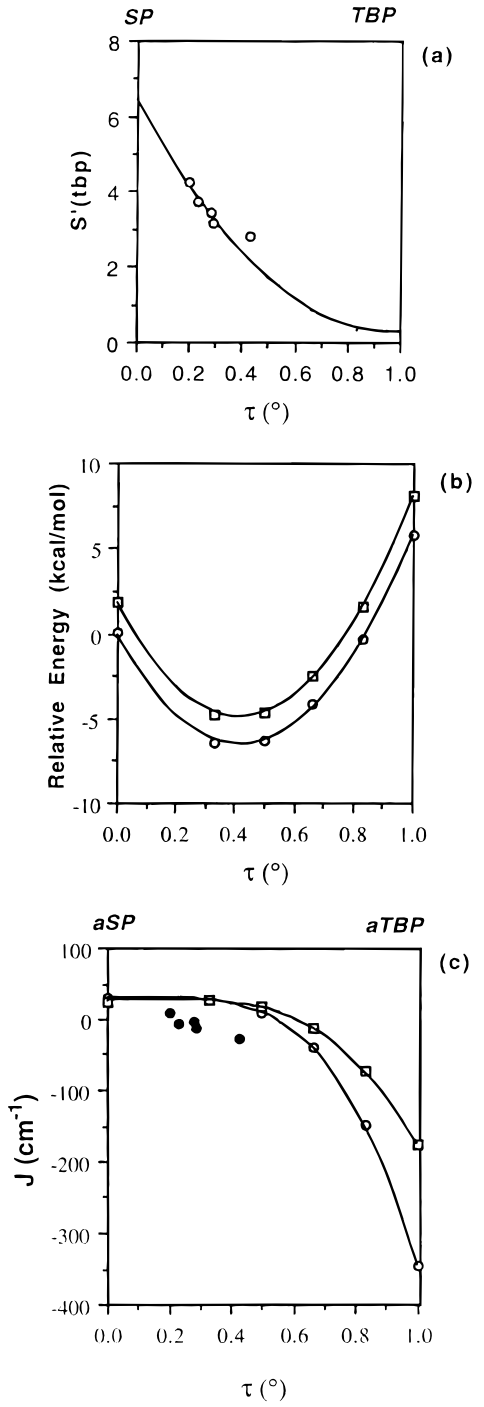

Figure 3. (a) Relationship between the angular parameter τ and the trigonal bipyramidal continuous-symmetry measure for the model compound $[Cu_2(\mu\text{-}N_3)_2(NH_3)_6]^{2+}$ along the Berry pathway (continuous line) and for the experimental structures (circles). (b) Calculated energy of $[Cu_2(\mu\text{-}N_3)_2(NH_3)_6]^{2+}$ in its lowest-energy spin state along the Berry pathway from a square pyramid ($\tau = 0$) to a trigonal bipyramid ($\tau = 1$). (c) Calculated exchange coupling constant J along the Berry coordinate, together with experimental values (closed circles). Calculated values are given for both a planar $Cu_2(N_3)_2$ ring ($\delta = 0°$, open circles) and a distorted ring ($\delta = 20°$, open squares).

pyramid are between 5.3 and 10.0, depending on the bond angles encompassed by axial and equatorial ligands. Also, for a large variety of homoleptic pentacoordinate complexes we found that a good correlation exists between τ and S(tbp).[23] In the present case, a good correlation is found between τ and S(tbp) for the model complex and also for the experimental data (Figure 3a). Therefore, we will use the angular parameter τ from here on, because similar plots are obtained if the symmetry measure is employed instead.

From the experimental data, a correlation between the experimental J and τ values was proposed,[3] according to which the value of J becomes more positive as τ increases. However, the range of reported experimental values is relatively limited and precludes drawing any firm conclusion. To verify the proposed magnetostructural correlation and extend it to a wider range of geometries, we have carried out calculations for the axially bridged model compound at different values of τ. Notice that the Berry type aSP to aTBP interconversion pathway chosen by us keeps the bridge−Cu−bridge angle constant (90°, as found in the experimental structures).

A plot of the energy of the ground state as a function of τ (Figure 3b) shows a minimum for an intermediate geometry ($\tau \approx 0.4$), but energy differences of less than 2 kcal/mol are predicted for structures in the range $0.2 \leq \tau \leq 0.6$, in excellent agreement with the experimental structures (Table 1, compounds **A**−**E**). We notice that similar results are obtained for the model with a planar ($\delta = 0°$) or puckered ($\delta = 20°$) Cu_2N_6 ring.

The calculated J values are represented in Figure 3c as a function of τ. These calculations have been carried out for both a planar ($\delta = 0°$) and a puckered ($\delta = 20°$, chair conformation) CuN_3CuN_3 ring. The coupling constant is seen to be little affected by deviations from the square pyramidal geometry up to $\tau \approx 0.5$, but drops sharply when approaching the trigonal bipyramid to give the strong antiferromagnetic coupling reported above for the regular aTBP structure (Table 2). The experimental values follow a similar trend, but the calculated J in the model compound is systematically more positive than that found experimentally for compounds with the same value of τ. One must be aware, though, that in experimental structures, parameters other than τ vary and might be responsible for the differences between calculated and experimental values. To verify whether the quantitative disagreement is due to the simplification consistent with varying only one structural parameter in a model compound or to the limitations of the computational approach, we report calculations on full structures in a later section.

Geometry Optimization. To test the importance that the arbitrary geometry choice for the model molecules has on the calculated J value, we carried out a partial geometry optimization for $[(NH_3)_3Cu(\mu\text{-}N_3)_2Cu(NH_3)_3]^{2+}$ with axially coordinated bridges using a starting geometry intermediate between aSP and aTBP and close to the experimental ones (i.e., the values of $\delta = 20°$ and $\tau = 0.33$ were kept frozen). The geometry optimization was carried out for both the broken symmetry and the high spin states, and the former was found at lower energy. Then, the energy of the high spin state was calculated with the optimized geometry of the broken symmetry state, and the optimized structural parameters are summarized in **6**. The

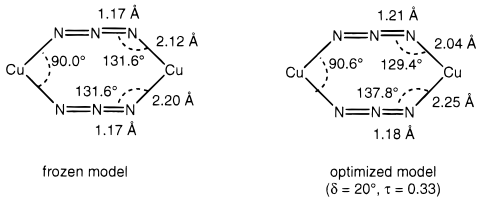

6

optimized structure is only 5.1 kcal mol^{-1} more stable than the starting one. Interestingly, the small structural differences between the starting structure and the optimized one (maximum

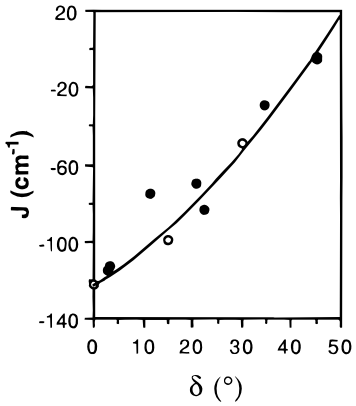

Figure 4. Calculated exchange coupling constant J (open circles) for $[Ni_2(\mu\text{-}N_3)_2(NH_3)_8]^{3+}$ as a function of the ring distortion parameter δ (see **4**). Experimental data (closed circles) are also shown for comparison.

deviations of 4.7% and 3.8% from the starting values for bond angles and distances, respectively) result in a shift of the coupling constant from 26.8 to -5.3 cm^{-1}, in good semiquantitative agreement with the experimental J of compounds **C** and **D** with similar values of δ and τ ($J_{exp} = -3.6$ and -7.5 cm^{-1}, respectively).

Calculations for Full Structures. As a final test, we have checked the ability of the computational methodology adopted by performing calculations for three complete structures, including the counterions. The results (Table 1) are in excellent agreement with the experimental data for compounds **E** and **F**. For compound **D**, however, the calculations agree with the experiment in the sense that the exchange coupling is weak, but they fail to reproduce the antiferromagnetic nature of the interaction. Although one must realize that the difference between calculated and experimental singlet−triplet gaps in this case is very small, this is the only case among a variety of theoretical studies carried out by us recently in which a calculated coupling constant for a complete structure has a different sign than that experimentally observed, from a total of 43 complexes belonging to 8 different families. We note, in addition, that the crystal structure was refined with disordered perchlorate ions, and the uncertainties thereof introduced in the atomic coordinates might bias the calculated J value.

Double-Bridged Ni(II) Complexes

To facilitate comparison with the above results on double-bridged Cu(II) compounds we discuss first the double-bridged Ni(II) complexes and then the single-bridged ones. Two main differences appear between the Cu and Ni complexes. On one hand, the Ni(II) compounds are always hexacoordinate, in contrast with the pentacoordination found for most Cu(II) complexes with end-to-end azido bridges. On the other hand, the Ni(II) ion has one more unpaired electron, and therefore the ferromagnetically coupled state has a total spin of $S = 2$.

The calculated values of J for the model complex $[Ni_2(\mu\text{-}N_3)_2(NH_3)_8]^{2+}$ as a function of the ring puckering are presented in Figure 4. In this case we have limited our study to the chair conformation, because all of the experimental structures appear in that conformation (Table 3). It can be seen that the coupling constant becomes less negative with the distortion, as computationally found above for Cu(II), a trend that was predicted by Ribas et al. based on the variation of the orbital gaps with δ in extended Hückel calculations.[24] The difference is that even for a large distortion the value of J remains negative in the Ni model complex, whereas for Cu positive values of J were found for large distortions (Figure 2). Even though the experimental data show some dispersion, they seem to follow the same trend (Figure 4).

Table 3. Structural Data (Angles in Degrees) and Experimental Exchange Coupling Constants (cm^{-1}) for Binuclear Ni(II) Complexes with Two End-to-End Azido Bridges

compound[a]	χ	δ	J_{exp}	refcode[c]	ref
$[Ni_2(\mu\text{-}N_3)_2(tren)_2](BPh_4)_2$	0	21	−70	ztanpb	25
$[Ni_2(\mu\text{-}N_3)_2(en)_2](PF_6)_2$	0	45	−4.6	latloh	24
$[Ni_2(\mu\text{-}N_3)_2(pn)_2](BPh_4)_2$	0	3	−114	latlun	24
$[Ni_2(\mu\text{-}N_3)_2(N_3)_2(tacd)_2]$	0	7	−90[b]	degsen	26
$[Ni_2(\mu\text{-}N_3)_2(N_3)_2(tmtacn)_2]$	32	16	−73	raxbun	2
$[Ni_2(\mu\text{-}N_3)_2(222\text{-}tet)_2](BPh_4)_2$	0	22	−84	niwyun	27
$[Ni_2(\mu\text{-}N_3)_2(2\text{-}ametpy)_2](PF_6)_2$	0	35	−29	zovlif	28
$[Ni_2(\mu\text{-}N_3)_2(hmcyclam)_2](ClO_4)_2$	0	3	−113	siwyec	29
$[Ni_2(\mu\text{-}N_3)_2(hmcyclam)_2](PF_6)_2$	0	13	−75	siwyig	29

[a] See ref 51 for abbreviations used in this table. Solvation molecules not included in the formulas. [b] The Hamiltonian employed was not specified. [c] Codes for locating structural data in the Cambridge Structural Database (ref 52).

Single-Bridged Ni(II) Complexes

For the single-bridged Ni complexes, we study first the effect of the deviation from linearity of the Ni−N_3−Ni skeleton, measured by the angle β (**1b**). Thus, a value of 0° for β corresponds to a linear skeleton. Our calculations predict weak antiferromagnetic coupling for compounds slightly distorted from linearity (β up to 30°), and a dramatic enhancement of the antiferromagnetism at larger values of β. Such a trend is in agreement with the angle dependence of the gap between the two MOs formed by the d_{z^2} orbitals reported by Escuer et al. from extended Hückel calculations.[30] The energy of the broken-symmetry singlet state presents its minimum at $\beta = 0°$ and is not very sensitive to the distortion. Hence, for $\beta = 40°$, the relative energy calculated for our model compound is only 3.4 kcal/mol. Because most of the experimental structures present values of β between 40 and 50° (Table 4), it seems likely that in the real molecules the linear conformation is destabilized by the repulsion between the substituents of the equatorial terminal ligands. In the two compounds that are closer to linearity[31,32]

(24) Ribas, J.; Monfort, M.; Díaz, C.; Bastos, C.; Solans, X. *Inorg. Chem.* **1993**, *32*, 3557.
(25) Pierpont, C. G.; Hendrickson, D. N.; Duggna, D. M.; Wagner, F.; Barefield, E. K. *Inorg. Chem.* **1975**, *14*, 604.
(26) Chaudhuri, P.; Guttman, M.; Ventur, D.; Wieghardt, K.; Nuber, B.; Weiss, J. *J. Chem. Soc., Chem. Commun.* **1985**, 1618.
(27) Escuer, A.; Castro, I.; Mautner, F.; El Fallah, M. S.; Vicente, R. *Inorg. Chem.* **1997**, *36*, 4633.
(28) Ribas, J.; Monfort, M.; Ghosh, B. K.; Cortés, R.; Solans, X.; Font-Bardia, M. *Inorg. Chem.* **1996**, *35*, 864.
(29) Escuer, A.; Vicente, R.; El Fallah, M. S.; Solans, X.; Font-Bardía, M. *Inorg. Chim. Acta* **1998**, *278*, 43.
(30) Escuer, A.; Vicente, R.; Ribas, J.; El Fallah, M. S.; Solans, X.; Font-Bardia, M. *Inorg. Chem.* **1993**, *32*, 3727.
(31) Fabrizzi, L.; Pallavicini, P.; Parodi, L.; Perrotti, A.; Sardone, N.; Taglietti, A. *Inorg. Chim. Acta* **1996**, *244*, 7.
(32) Escuer, A.; Harding, C. J.; Dussart, Y.; Nelson, J.; McKee, V.; Vicente, R. *J. Chem. Soc., Dalton Trans.* **1999**, 223.
(33) McLachlan, G. A.; Fallon, G. D.; Martin, R. L.; Moubaraki, B.; Murray, K. S.; Spiccia, L. *Inorg. Chem.* **1994**, *33*, 4663.
(34) Wagner, F.; Mocella, M. T.; D'Aniello, M. J., Jr.; Wang, A. H.-J.; Barefield, E. K. *J. Am. Chem. Soc.* **1974**, *96*, 2625.
(35) Escuer, A.; Vicente, R.; Ribas, J.; El Fallah, M. S.; Solans, X.; Font-Bardia, M. *Inorg. Chem.* **1994**, *33*, 1842.
(36) Ribas, J.; Monfort, M.; Díaz, C.; Bastos, C.; Mer, C.; Solans, X. *Inorg. Chem.* **1995**, *34*, 4986.

Table 4. Experimental Structural Data and Exchange Coupling Constants[a] for Ni(II) Binuclear Complexes with One End-to-End Azido-Bridge, and for Analogous Chain Complexes with Two End-to-End Azido-Bridges

compound[b]	type	β	J_{exp}	refcode[d]	ref
$[Ni_2(\mu\text{-}N_3)(trenpy)_2](ClO_4)_3$	binuclear	48.4	−54	lijcuc	33
$[Ni_2(\mu\text{-}N_3)(crypt)](N_3)(ClO_4)$	binuclear	12.8		tazwia	31
$[Ni(\mu\text{-}N_3)(H_2O)(crypt)](CF_3SO_3)_2$	binuclear	18.3	+12	jocdua	32
$[Ni_2(\mu\text{-}N_3)(Me_4cyclam)_2]_nI_n$	binuclear	40.4	−25	aztdni	25, 34
$[Ni_2(\mu\text{-}N_3)(333\text{-tet})]_n(PF_6)_n$	cis chain	28.5	−18	pitmek	35
$[Ni_2(\mu\text{-}N_3)(men)_2]_n(ClO_4)_n$	cis chain	51.1	−17	zolliv	36
$[Ni_2(\mu\text{-}N_3)(men)_2]_n(PF_6)_n$	cis chain	51.2	−3.2	zollob	36
$[Ni_2(\mu\text{-}N_3)(2\text{-ametpy})_2]_n(ClO_4)_n$	cis chain	52.9	−1.0	zovleb	28
$[Ni_2(\mu\text{-}N_3)(bipy)_2]_n(ClO_4)_n$	cis chain	57.1	−33	hewnec	37
$[Ni_2(\mu\text{-}N_3)(bipy)_2]_n(PF_6)_n$	cis chain	57.4	−22	hewnig	37
$[Ni_2(\mu\text{-}N_3)(Me_2tn)_2]_n(ClO_4)_n$	trans chain	42.8	−49		38
$[Ni_2(\mu\text{-}N_3)(dmpn)_2]_n(PF_6)_n$	trans chain	43.4	−41 (HT)[c] −19 (LT)[c]	rellez	39
$[Ni_2(\mu\text{-}N_3)(mpz)_4]_n(ClO_4)_n$	trans chain	42.6	+6.9	hecqah	40
$[Ni_2(\mu\text{-}N_3)(cyclam)]_n(ClO_4)_n$	trans chain	45.5	−39	juxyac	6
$[Ni_2(\mu\text{-}N_3)(hmcyclam)_2]_n(ClO_4)_n$	trans chain	50.4 48.5	−41 −36	wibdam	41
$[Ni_2(\mu\text{-}N_3)(333\text{-tet})]_n(ClO_4)_n$	trans chain	47.0	−81	pitmag	35
$[Ni_2(\mu\text{-}N_3)(232\text{-tet})]_n(ClO_4)_n$	trans chain	50.7	−27	hakjuy	30
$[Ni_2(\mu\text{-}N_3)(323\text{-tet})]_n(ClO_4)_n$	trans chain	52.2	−63	hakkaf	30
$[Ni_2(\mu\text{-}N_3)(tmd)_2]_n(PF_6)_n$	trans chain	53.9	−71 (HT)[c] −56 (LT)[c]	rellid	39
$[Ni_2(\mu\text{-}N_3)(tmd)_2]_n(ClO_4)_n$	trans chain	59.1	−100		38
$[Ni_2(\mu\text{-}N_3)(dmcyclen)]_n(ClO_4)_n$	trans chain	60.3	−101	wibdiu	41
$[Ni_2(\mu\text{-}N_3)(Me_2cyclen)]_n(ClO_4)_n$	trans chain	63.0	−98	yogjuz10	42

[a] All angles in deg; coupling constants in cm^{-1}. [b] See ref 51 for abbreviations used in this table. Solvation molecules not included in the formulas. [c] LT = low-temperature phase; HT = high-temperature phase. [d] Codes for locating structural data in the Cambridge Structural Database (ref 52).

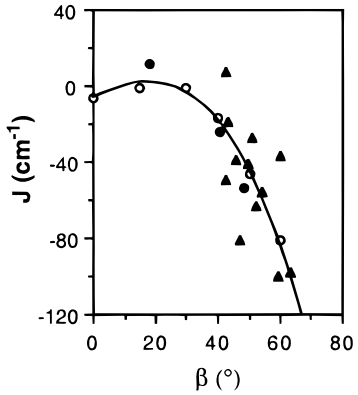

Figure 5. Calculated exchange coupling constant J (open circles) for $[Ni_2(\mu\text{-}N_3)(NH_3)_{10}]^{3+}$ and experimental data for binuclear complexes (closed circles) and trans chain complexes $\{[Ni(\mu\text{-}N_3)(NH_3)_4]^{2+}\}_n$ (closed triangles).

($\beta \approx 13°$), a cryptand ligand substitutes those interligand repulsions by chemical bonds, thus allowing for the electronically preferred linear geometry to show up.

The general behavior of the experimental data for binuclear complexes (Figure 5, closed circles) seems to be in agreement with the calculated values for the model compound, although the limited number of experimental data precludes at the present time a full verification of the predicted dependence of J on the bond angle. A larger number of data is available for analogous chain compounds. If one considers that the magnetic behavior of those chains is mainly dictated by the nearest-neighbor interactions, their experimentally deduced J values can be plotted along with our theoretical results (Figure 5, closed triangles for trans chains), indicating an excellent agreement between theory and experiment. The experimental data for cis chains (Table 4), on the other hand, are in semiquantitative agreement with the calculations, but do not seem to give a clear magnetostructural correlation as predicted in Figure 5. A case worth discussing in more detail is that of the practically linear ($\beta = 13°$) complex reported by Escuer et al., for which our model calculations would predict a J value close to zero (Figure 6) in contrast with the clear ferromagnetic behavior found experimentally ($J_{exp} = +11.8\ cm^{-1}$). The disagreement in this case should not be interpreted as a failure of the theoretical predictions. A look at the molecular structure of such a compound tells us that one of the Ni atoms is pentacoordinate, in contrast with the hexacoordination adopted in our model molecule and found in all of the other experimental structures (Table 4). A calculation on a model of that complex, in which the macrocyclic ligands are substituted by monodentate NH_3 groups, gives a J value of $+7.6\ cm^{-1}$, in fair agreement with the experimental value ($+11.8\ cm^{-1}$). If, however, the two Ni atoms in such a model are made hexacoordinate, with four NH_3 and one H_2O terminal ligands each, the calculated J is $+2.8\ cm^{-1}$, consistent with the expectations for our model with five NH_3 ligands at $\beta = 13°$ (Figure 5). These results can be interpreted as an indication that the ferromagnetism in the compound reported by Escuer et al. is most likely due to the pentacoordination of one of the Ni atoms, rather than to the almost linear $Ni-N_3-Ni$ framework.

For the Ni(II) complexes with one bridging azido ligand, the analysis of the orbital energies shows that the two combinations of the d_{z^2} orbitals are practically degenerate. In contrast, the $d_{x^2-y^2}$ orbitals are separated by a small energy gap (of about $10^4\ cm^{-1}$), as found for the Cu(II) compounds with double bridges, that increases when the linearity is lost (Figure 6a). It

(37) Cortés, R.; Urtiaga, K.; Lezama, L.; Pizarro, J. L.; Goñi, A.; Arriortúa, M. I.; Rojo, T. *Inorg. Chem.* **1994**, *33*, 4009.
(38) Ribas, J.; Escuer, A.; Monfort, M.; Vicente, R.; Cortés, R.; Lezama, L.; Rojo, T. *Coord. Chem. Rev.* **1999**, *193−195*, 1027.
(39) Monfort, M.; Ribas, J.; Solans, X.; Font-Bardia, M. *Inorg. Chem.* **1996**, *35*, 7633.
(40) Hong, C. S.; Do, Y. *Angew. Chem., Int. Ed.* **1999**, *38*, 193.
(41) Escuer, A.; Vicente, R.; El Fallah, M. S.; Ribas, J.; Solans, X.; Font-Bardia, M. *J. Chem. Soc., Dalton Trans.* **1993**, 2975.
(42) Vicente, R.; Escuer, A.; Ribas, J.; El Fallah, M. S.; Solans, X.; Font-Bardia, M. *Inorg. Chem.* **1995**, *34*, 1278, 5096.

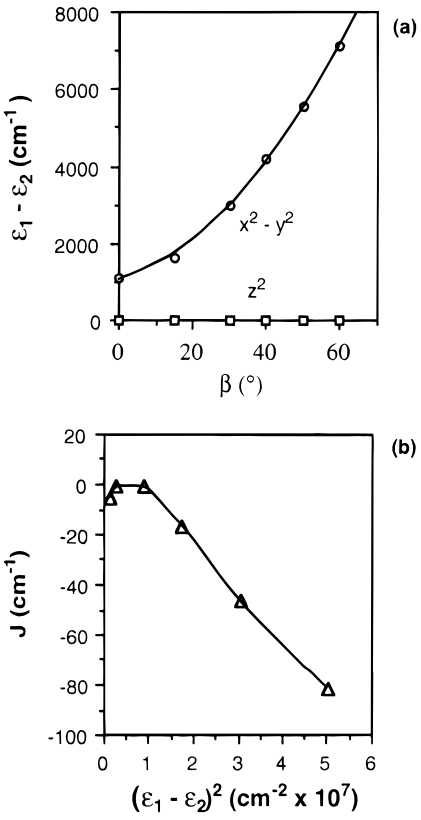

Figure 6. (a) Orbital energy gaps for the pairs of SOMOs that contain the symmetric (A_g) and antisymmetric (B_u) combinations of the $d_{x^2-y^2}$ (circles) and d_{z^2} (squares) orbitals calculated for $[Ni_2(\mu\text{-}N_3)(NH_3)_{10}]^{3+}$ as a function of the bond angle β (**1**). (b) Calculated values of the coupling constant J as a function of the calculated energy gap between the $d_{x^2-y^2}$ SOMOs.

is noteworthy that an excellent linear correlation is found between the calculated J values and the squared orbital gap of the metal $d_{x^2-y^2}$ orbitals $(\epsilon_1 - \epsilon_2)^2$, except for the very small gaps that result for an almost linear arrangement of the Ni−N_3−Ni backbone (Figure 6b). Such result is similar to the one discussed above for double-bridged Cu(II) complexes, and indicates that the structural dependence of the exchange coupling in the presently studied Ni(II) complexes is practically governed by the $d_{x^2-y^2}$ orbital gap.

Acknowledgment. This work was supported by DGES through project number PB98-1166-C02-01. Partial support of this research came from the Training and Mobility of Researchers Program, Access to Large Installations, under contract ERBFMGECT950062, Access to Supercomputing Facilities for European Researchers, established between the European Community and CESCA-CEPBA. The authors are indebted to A. Escuer for many clarifying discussions.

Appendix: Computational Details

The exchange coupling constant J for the azido-bridged binuclear complexes has been estimated by calculating the energy difference between the high spin (HS) state and the broken-symmetry singlet (BS) solution (assuming the spin Hamiltonian is defined as $H = -J\mathbf{S}_1\cdot\mathbf{S}_2$), according to the following expression

$$J = 2\,\frac{E_{BS} - E_{HS}}{S(S+1)} \qquad (2)$$

Table 5. Structural Parameters Used for the Calculations on the Model Complex $[(NH_3)_3Cu(\mu\text{-}N_3)_2Cu(NH_3)_3]$[a]

	eSP	aSP	eTBP	eTBP
Cu−N^{eq}	2.00	2.00	2.00	2.00
Cu−N^{ax}	2.00	2.40	2.25	2.00
N1−Cu−N3	90	90	90	120
N2−N3−Cu	131.4	131.4	131.4	120
N2−N1−Cu	138.6	138.6	138.6	120
N1−N2	1.17	1.17	1.17	1.17
Cu···Cu	5.17	5.46	5.35	4.34
N−H	0.98	0.98	0.98	0.98

[a] All distances in Å, angles in deg.

where S corresponds to the total spin of the high spin state. Note that the energy of the broken-symmetry solution is taken as an approximation to that of the singlet state.[43] Such an approach has been shown by us to give values for unmodelized molecules that are in excellent agreement with the experimental data for complexes with different first row transition metal ions.[8,16,18,44,45] The reader must be aware, however, that other authors have employed an expression for the coupling constant originally proposed by Noodleman that mimics a procedure based on a Hartree−Fock determinant,[46] which would yield larger absolute values of J (up to 2 times larger for Cu(II), and 1.5 times larger for Ni(II)) than those reported here. The choice of either approach has thus no major significance for the qualitative description of the magnetostructural correlations.

All calculations were carried out with the help of the Gaussian 94 program[47] using the hybrid B3LYP method proposed by Becke.[48] In a previous paper,[44] after evaluating several functionals, we found that the B3LYP method combined with the broken-symmetry approach provides the best results for the calculation of coupling constants. For model structures we have carried out the calculations using an all-electron double-ζ basis set,[49] whereas for the complete structures a triple-ζ basis set was used for the metal atom.[50] The two-electron integrals in the MO basis have been computed using the standard four index transformation implemented in Gaussian, modified for our case

(43) Ruiz, E.; Cano, J.; Alvarez, S.; Alemany, P. *J. Comput. Chem.* **1999**, *20*, 1391.
(44) Ruiz, E.; Alemany, P.; Alvarez, S.; Cano, J. *J. Am. Chem. Soc.* **1997**, *119*, 1297.
(45) Ruiz, E.; Alemany, P.; Alvarez, S.; Cano, J. *Inorg. Chem.* **1997**, *36*, 3683.
(46) Noodleman, L.; Case, D. A. *Adv. Inorg. Chem.* **1992**, *38*, 423.
(47) Frisch, M. J.; Trucks, G. W.; Schlegel, H. B.; Gill, P. M. W.; Johnson, B. G.; Robb, M. A.; Cheeseman, J. R.; Keith, T.; Petersson, G. A.; Montgomery, J. A.; Raghavachari, K.; Al-Laham, M. A.; Zakrzewski, V. G.; Ortiz, J. V.; Foresman, J. B.; Cioslowski, J.; Stefanov, B. B.; Nanayakkara, A.; Challacombe, M.; Peng, C. Y.; Ayala, P. Y.; Chen, W.; Wong, M. W.; Andres, J. L.; Replogle, E. S.; Gomperts, R.; Martin, R. L.; Fox, D. J.; Binkley, J. S.; Defrees, D. J.; Baker, J.; Stewart, J. J. P.; Head-Gordon, M.; Gonzalez, C.; Pople, J. A., *Gaussian 94*, Gaussian, Inc.: Pittsburgh, PA, 1995.
(48) Becke, A. D. *J. Chem. Phys.* **1993**, *98*, 5648.
(49) Schaefer, A.; Horn, H.; Ahlrichs, R. *J. Chem. Phys.* **1992**, *97*, 2571.
(50) Schaefer, A.; Huber, C.; Ahlrichs, R *J. Chem. Phys.* **1994**, *100*, 5829.
(51) Abbreviations: ametpy = 2-aminoethyl-pyridine; bipy = 2,2′-bipyridine; cyclam = 1,4,8,11-tetraazacyclotetradecane; crypt = $N[(CH_2)_2\text{-}NHCH_2\text{-}(C_6H_4)CH_2NH(CH_2)_2]_3N$; dien = diethylenetriamine; dmcyclen = 2,3-dimethyl-1,4,8,11-tetraazacyclotetradecane-1,3-diene; hmcyclam = 5,5,7,12,12,14-hexamethyltetraazacyclotetradecane; men = 1,2-diamino-2-methylpropane; mpz = 5-methylpyrazole; pn = 1,3-diamino-propane; tacd = 1,5,9-triazacyclododecane; 222-tet = *N*,*N*′-bis(2-aminoethyl)-1,2-propanediamine; 232-tet = *N*,*N*′-bis(2-aminoethyl)-1,3-propanediamine; 323-tet = *N*,*N*′-bis(3-aminoethyl)-1,2-propanediamine; 333-tet = *N*,*N*′-bis(3-aminoethyl)-1,3-propanediamine; tmd = 1,3-diamino-2,2-dimethylpropane; tmtacn = 1,4,7-trimethyl-1,4,7-triazacyclononane; tn = 2,2′-dimethyl-1,3-diaminopropane; tren = 2,2′,2″-triaminotriethylamine; trenpy = *N*,*N*-bis(2-aminoethyl)-*N*′-(2-pyridylmethyl)ethane-1,1-diamine.
(52) Allen, F. H.; Kennard, O. *Chem. Des. Autom. News* **1993**, *8*, 31.

in a specific link attached to the program, designed to make the disk storage as small as possible.

Several test calculations were carried out to investigate whether other structural parameters could affect the value of J and the following results were obtained:

(1) The asymmetry of the azido ligands, given by the difference between the two nonequivalent N−N bond distances, was changed in the axially bridged $[(NH_3)_3Cu(\mu\text{-}N_3)_2Cu(NH_3)_3]$ model with $\tau = 0.5$ and $\delta = 20°$. A difference of up to 0.2 Å between the two distances (keeping the sum constant) results in differences smaller than 1 cm^{-1} in the calculated J.

(2) Substitution of the hydrogen atoms by methyl groups in the terminal ligands for the axially linked Cu(II) model with $\tau = 0.33$ and $\delta = 20°$ resulted in a shift of the calculated J from -17.5 to $+25.8$ cm^{-1}.

(3) Changes in the N−Cu−N bond angle with the azido bridges changes from 90 to 95 to 100° result in calculated J values of -17.5, $+37.3$, and $+44.8$ cm^{-1}, respectively.

(4) Varying the Cu−N−N bond angles by up to 13° does not significantly affect the calculated J (again the axially bridged model with $\tau = 0.3$ and $\delta = 20°$ was used).

The relevant bond distances and angles used in the model calculations of Cu(II) complexes are collected and presented in Table 5. The following parameters were used for the calculations on Ni(II) complexes: Ni−N (N_3) = 2.15, Ni−N (NH_3) = 2.10, N−N = 1.18, and N−H = 1.0 Å; N−Ni−N = 90°, and Ni−N−N = 135° in double-bridged complexes.

IC000005X